Neurochemistry International 124 (2019) 181–192

Contents lists available at ScienceDirect

Neurochemistry International

journal homepage: www.elsevier.com/locate/neuint

# Protocatechuic acid improves functional recovery after spinal cord injury by attenuating blood-spinal cord barrier disruption and hemorrhage in rats

Chan Sol Park[a,b], Jee Youn Lee[a], Hae Young Choi[a], Bong Gun Ju[c], Inchan Youn[b,d,e,*], Tae Young Yune[a,b,f,**]

[a] Age-Related and Brain Diseases Research Center, Kyung Hee University, Seoul, 02447, Republic of Korea
[b] KHU-KIST Department of Converging Science and Technology, Kyung Hee University, Seoul, 02447, Republic of Korea
[c] Department of Life Science, Sogang University, Seoul, 04107, Republic of Korea
[d] Biomedical Research Institute, Korea Institute of Science and Technology, 5, Hwarang-ro 14-gil, Seongbuk-gu, Seoul, 02791, Republic of Korea
[e] Department of Biomedical Engineering, Korea University of Science and Technology, 217, Gajeong-ro, Yuseong-gu, Daejeon, 34113, Republic of Korea
[f] Department of Biochemistry and Molecular Biology, School of Medicine, Kyung Hee University, Seoul, 02447, Republic of Korea

ARTICLE INFO

*Keywords:*
Protocatechuic acid
Blood-spinal cord barrier
Spinal cord injury
Hemorrhage
Matrix metalloprotease

ABSTRACT

After spinal cord injury (SCI), blood-spinal cord barrier (BSCB) disruption and hemorrhage lead to blood cell infiltration and progressive secondary injuries including inflammation. Inflammatory response is one of the major events resulting in apoptosis, scar formation and neuronal dysfunction after SCI. Here, we investigated whether protocatechuic acid (PCA), a natural phenolic compound, would attenuate BSCB disruption and hemorrhage, leading to functional improvement after SCI. After a moderate contusion injury at T9, PCA (50 mg/kg) was administrated via intraperitoneal injection immediately, 6 h, and 12 h after SCI, and the same dose of PCA once a day until 7 d after injury. Our data show that PCA inhibited apoptotic cell death of neurons and oligodendrocytes and improved functional recovery after injury. PCA also attenuated BSCB disruption and hemorrhage and reduced the infiltration of neutrophils and macrophages compared to vehicle control. Moreover, PCA inhibited the expression and activation of matrix metalloprotease-9, which is well known to disrupt BSCB after SCI. Furthermore, PCA treatment significantly inhibited the expression of sulfonylurea receptor 1 and transient receptor potential melastatin 4, which are known to mediate hemorrhage at an early stage after SCI. Consistent with these findings, the mRNA and protein expression of inflammatory mediators such as tumor necrosis factor alpha, interleukin 1 beta, cyclooxygenase-2, inducible nitric oxide synthase, and chemokines was significantly alleviated by PCA treatment. Thus, our results suggest that PCA improved functional recovery after SCI in part by inhibiting BSCB disruption and hemorrhage through the down-regulation of sulfonylurea receptor 1/transient receptor potential melastatin 4 and matrix metalloprotease-9.

## 1. Introduction

Spinal cord injury (SCI) is one of the most severe traumatic injuries that result in dysfunction of limb and trunk below the damaged region, leading to spinal cord edema and cell death in the injured areas and even permanent disability. The primary mechanical injury causes axonal and vascular damage at the lesion site and then a series of pathological events are initiated in response to a primary injury to further impair the wound site and its surrounding regions. These vascular events, including changes in blood flow, intraspinal hemorrhage, and blood-spinal cord barrier (BSCB) destruction, are important factors causing secondary damage, thereby resulting in chronic permanent dysfunction after SCI (Garcia et al., 2016; Sinescu et al., 2010). After BSCB disruption, blood cells such as neutrophils and macrophages are infiltrated into the injured parenchyma and produce inflammatory mediators such as pro-inflammatory cytokines and chemokines, contributing to secondary injuries (Abbott et al., 2006; Hausmann, 2003; Hawkins and Davis, 2005; Zlokovic, 2008). The inflammation is one of the major event of secondary injuries and plays a central role in regulating the pathogenesis of acute and chronic SCI (Genovese et al.,

* Corresponding author. Biomedical Research Institute, Korea Institute of Science and Technology, 5, Hwarang-ro 14-gil, Seongbuk-gu, Seoul, 02791, Republic of Korea.
** Corresponding author. Department of Biochemistry and Molecular Biology and Age-Related and Brain Diseases Research Center, School of Medicine, Kyung Hee University, Medical Building 10th Floor, Dongdaemun-gu, Hoegi-dong 1, Seoul, 02447, Republic of Korea.
*E-mail addresses:* iyoun@kist.re.kr (I. Youn), tyune@khu.ac.kr (T.Y. Yune).

https://doi.org/10.1016/j.neuint.2019.01.013
Received 19 October 2018; Received in revised form 4 January 2019; Accepted 14 January 2019
Available online 18 January 2019
0197-0186/ 

2009; Hausmann, 2003). Particularly, the inflammatory responses are implicated in neurons and oligodendrocytes cell death, scar formation and the reduction of neuronal function (Garcia et al., 2016; Keane et al., 2006; Zhang et al., 2012). Thus, it is believed that the attenuation of inflammatory response by inhibiting BSCB disruption could be an effective therapeutic strategy by reducing secondary degeneration followed functional deficit after SCI.

Protocatechuic acid (PCA, 3, 4-dihydroxybenzoic acid), a simple phenolic compound, abundant in edible vegetables, fruits, nuts and herbal medicines has numerous biological activities (Masella et al., 2012; Yin et al., 2015). PCA is also known to have anti-viral, antioxidant, anti-inflammatory, anti-platelet and anti-tumor effects *in vivo* and *in vitro* (Lin et al., 2011; Tsao et al., 2014). Recently, the neuroprotective effect of PCA has been reported in several central nervous system (CNS) diseases animal models such as chronic intermittent hypoxia, depression, seizure, Parkinson's disease (PD), Alzheimer's disease (AD), and brain trauma. For example, PCA protected and preserved hippocampal, dopaminergic, and cortical neurons in pilocarpine induced epileptic seizures, 1-methyl-4-phenyl-1,2,3,6-tetrahydropyridine-induced PD model, and traumatic brain injury model (Lee et al., 2017, 2018b; Zhang et al., 2010). PCA also inhibited the aggregation of β-amyloid and α-synuclein closely related to AD and PD (Guan et al., 2006; Shi et al., 2006). In addition, PCA ameliorated cognitive functions impairment and neuronal apoptosis in hippocampus and prefrontal cortex following chronic intermittent hypoxia exposure in rat (Yin et al., 2015) and exhibited antidepressant like effect by inhibiting oxidative damage in the cerebral cortex and hippocampus induced by acute restraint stress in mice (Thakare et al., 2017). Thus, based on these results, we hypothesized that PCA might exhibit neuroprotective effects after SCI and examined whether PCA would alleviate neurons and oligodendrocytes cell death, inhibit BSCB disruption and hemorrhage, and attenuate the expression of matrix metalloprotease (MMP) and sulfonylurea receptor 1 (SUR1)/transient receptor potential melastatin 4 (TrpM4) and thereby improve functional recovery.

## 2. Materials and methods

### 2.1. Animals and spinal cord injury

Adult rats [Sprague–Dawley; male; 250–300 g; Sam:TacN (SD) BR, Samtako, Osan, Korea] were housed at 20–24 °C on a 12 h light/dark cycle with food and water available ad libitum. Rats were housed one per cage (410 × 282 × 153 mm, transparent polycarbonate) with aspen shaving bedding and were fed a commercial diet (5L79, PMI Nutrition International, St Louis, MO). Rats were anesthetized with chloral hydrate (500 mg/kg) and moderate contusion injury (10 g × 25 mm) was made at the T9-T10 level using the New York University impactor as previously described (Lee et al., 2010, 2012a). For sham–operated controls, rats underwent a T10 laminectomy without weight-drop injury. Throughout the surgical procedure, body temperature was maintained at 37 ± 0.5 °C with a heating pad (Biomed S.L., Alicante, Spain). After SCI, muscles and skin were closed in layers, and rats were placed in a temperature and humidity-controlled chamber overnight. Postoperatively, rats were received subcutaneously supplemental fluids (5 ml, lactated ringer), analgesic (ketoprofen, 5 mg/kg) and antibiotics (gentamicin, 5 mg/kg) once daily for 5 d after surgery. Rats were housed one per cage after injury with water and food easily accessible. Body weights and the remaining chow and water weight were recorded each morning and the bladder was emptied manually three times per day until reflexive bladder emptying was established. All surgical interventions and post-operative animal care were performed in accordance with the Guidelines and Policies for Rodent Survival Surgery provided by the Animal Care Committee of the Kyung Hee University (Permission number: KHUASP(SE)-17-059).

### 2.2. Drug treatment

PCA (Cayman chemical, Ann Arbor, MI) was dissolved in 0.2% dimethyl sulfoxide in 0.9% saline and rats were given PCA immediately after SCI via intraperitoneal injection (i.p.) and received the same dose of PCA at 6 h and 12 h, and then treated once a day for 7 days. The preliminary study showed that a dose of 50 mg/kg of PCA was an optimal dose for recovery of hind limb locomotion after SCI (Supplementary Fig. 1). Therefore, 50 mg/kg of PCA was used in this study. Sham-operated control rats did not receive any pharmacological treatment. Vehicle group received 0.2% dimethyl sulfoxide in 0.9% saline.

### 2.3. Evans blue assay

To determine BSCB permeability, rats were injected with 5 ml of 2% Evans blue dye (Sigma-Aldrich, St. Louis, MO) at 1 d after injury and then rats were sacrificed 3 h later. Evans blue dye extravasation was measured as previously described (Lee et al., 2012a).

### 2.4. Spectrophotometric assay for intraspinal hemorrhage

At 24 h after injury, rats were sacrificed via cardiac puncture with heparinized saline to remove intravascular blood, and the hemoglobin content in the injured spinal cord tissue (5 mm segments of cord encompassing the lesion site) was measured with a spectrophotometric assay as described previously (Lee et al., 2015a; Simard et al., 2010) (n = 5 rats/group).

### 2.5. Tissue preparation

Rats were anesthetized with chloral hydrate and perfused via cardiac puncture initially with 0.1 M PBS and subsequently with 4% paraformaldehyde in 0.1 M PBS at indicated time points after SCI. For molecular work, rats were perfused with 0.1 M PBS and the spinal cord (10 mm) segments including lesion site were isolated and frozen at −80 °C as previously described (Lee et al., 2010) (n = 3 rats/group for each time point).

### 2.6. Immunohistochemistry

Frozen sections were processed for immunohistochemistry with antibodies against myeloperoxidase (MPO; 1:100; Dako, Carpinteria, CA), ED-1 (1:1000; Serotec, Raleigh, NC), cleaved caspase-3 (1:100; Cell Signaling Technology, Danvers, MA) and CC1 (1:100; Millipore, Billerica, MA) as previously described (Lee et al., 2014). For quantification of MPO or ED-1 intensity, serial transverse sections (20 μm thickness) were collected every 100 μm section rostral and caudal 3000 μm to the lesion site (total 60 sections). Digital images of tissues stained with MPO- or ED-1 antibodies were obtained using MetaMorph software (Molecular devices) to quantify and averaged the total fluorescence intensity of each cross-section exceeding the threshold. For double labeling, fluorescein isothiocyanate (FITC)- or cyanine 3-conjugated secondary antibodies (Jackson Immunoresearch, West Grove, PA) was used. Also, nuclei were labeled with DAPI according to the manufacturer's protocol (Invitrogen, Carlsbad, CA). For quantification of cleaved caspase-3-positive oligodendrocytes (cleaved caspase-3/CC1 double positive) was assessed according to the previous report (Lee et al., 2015b). Serial sections were stained with Cresyl violet acetate for histological analysis (n = 3 rats/group).

### 2.7. Cell counting of viable ventral motor neuron (VMN)

One day after injury, serial spinal cord sections were stained with Cresyl violet acetate. The number of viable VMN was manually counted from each field and analyzed by MetaMorph software (Molecular

devices) (n = 3 rats/group). The criteria for VMN counting was based on the previous report (Lee et al., 2014).

### 2.8. TUNEL staining

One and five days after injury, serial spinal cord sections were collected every 200 μm and processed TUNEL staining according to the manufacturer's instructions (ApopTag in situ kit, Millipore). A DAB substrate kit (Vector Laboratories, Burlingame, CA) was used for peroxidase staining. Control sections were treated similarly, but incubated in the absence of TDT enzyme, dUTP-digoxigenin, or antidigoxigenin Ab, and positive control sections were incubated in DNase I. TUNEL-positive cells in the gray matter (GM) at 1 d (total 40 sections) and in the white matter (WM) at 5 d (total 100 sections) after SCI were counted and quantified using a 20× objective. Only those cells showing morphological features of nuclear condensation and/or compartmentalization in the GM and WM were counted as TUNEL-positive (n = 5 rats/group).

### 2.9. RNA isolation and RT-PCR

Total RNA was isolated from spinal cord segments (10 mm), centered at the lesion site by using TRIZOL reagent (Invitrogen) and RT-PCR was performed as previously described (Yune et al., 2007). The primers used for RT-PCR were synthesized by Genotech (Daejeon, Korea), and the sequences of all primers are presented in Table 1 (n = 3 rats/group).

### 2.10. Western blot

Total protein from spinal cord segments was prepared and Western blot analysis was performed as previously described (Lee et al., 2012a). The primary antibodies used in Western blot are as follow. Zonula occludens-1 (ZO-1, 1:1000; Invitrogen), occludin (1:1000; Invitrogen), SUR1 (1:1000; Santa Cruz Biotechnology, Santa Cruz, CA), TrpM4 (1:1000; Santa Cruz Biotechnology), cleaved caspase-3 (1:1000; Cell Signaling Technology), ED-1 (1:200; Serotec), inducible nitric oxide synthase (iNOS, 1:1000; Transduction Laboratory, Lexington, KY), and cyclooxygenase-2 (COX-2, 1:1000; Cayman chemical), As loading control, β-tubulin (1:30,000; Sigma) was used. The primary antibodies were detected with a horseradish peroxidase-conjugated secondary antibody (Jackson ImmunoResearch). Immunoreactive bands were visualized by chemiluminescence using Supersignal (Thermo Scientific, Rockford, IL). The densitometric values of the bands on Western blots obtained by AlphaImager software (Alpha Innotech Corporation) were subjected to statistical analysis. Background in films was subtracted from the optical density measurements. Western blot analysis was assessed at the indicated time points (n = 3 rats/group).

### 2.11. Gelatin zymography

Because our previous report showed that the activity of MMP-2 and MMP-9 is maximized at 12–24 h after SCI, we examined the MMP-2 and MMP-9 activities at 1 d post-injury by gelatin zymography as described previously with some modification (Lee et al., 2012b). Total protein was loaded on a Novex 10% zymogram gel (EC61752; Invitrogen) and separated by electrophoresis. The gel was incubated with 2.5% Triton X-100 and then incubated with developing buffer (50 mM Tris-HCl, pH 8.5, 0.2 M NaCl, 5 mM $CaCl_2$, 0.02% Brii35) at 37 °C for 24 h, the gel was stained with 0.5% Coomassie and then destained. The clear bands on the zymogram were indicative of gelatinase activity (n = 3 rats/group).

### 2.12. Behavioral tests

Behavioral analyses including Basso–Beattie–Bresnahan (BBB) locomotion scale, Inclined plane test, grid walk test, and foot print analysis were conducted as previously described (Yune et al., 2007). BBB locomotion scale and inclined plane test were performed once a week as previously described (Basso et al., 1995; Rivlin and Tator, 1977; Yune et al., 2007). At 35d after SCI, grid walk test and foot print analysis were also assessed as previously described (Merkler et al., 2001; Stirling et al., 2004) (n = 10 rats/group). Behavioral analyses were performed by trained investigators who were blind as to the experimental conditions.

**Table 1**
Nucleotide sequences of primers and conditions used for RT-PCR.

| Target | Primer | Sequence | Annealing temperature (°C) | Cycles |
|---|---|---|---|---|
| MMP-2 | Forward | 5′-ACCGTCGCCCATCATCAA-3′ | 55 | 40 |
| | Reverse | 5′-TTGC ACTGCCAACTCTTTGTCT-3′ | | |
| MMP-9 | Forward | 5′-TCGAAGGCG ACCTCAAGTG-3′ | 55 | 40 |
| | Reverse | 5′-TTCGGTGTAGCTT TGGATCCA-3′ | | |
| Abcc8 | Forward | 5′-CCTGCAGCCAGACATAGACA -3′ | 61 | 35 |
| | Reverse | 5′-CAGTCAGCATGAGGCAGGTA-3′ | | |
| TrpM4 | Forward | 5′-CAGCGACCTCTACTGGAAGG-3′ | 62 | 35 |
| | Reverse | 5′-TCACGAGCTTGTGCCAATAG-3′ | | |
| IL-1β | Forward | 5′-GCAGCTACCTATGTCTTGCCCGTG-3′ | 52 | 30 |
| | Reverse | 5′-GTCGTTGCTTGTCTCTCCTTGTA-3′ | | |
| TNF-α | Forward | 5′-CCCAGACCCTCACACTCAGAT-3′ | 60 | 33 |
| | Reverse | 5′-TTGTCCCTTGAAGAGAACCTG-3′ | | |
| COX-2 | Forward | 5′-CCATGTCAAAACCGTGGTGAATG-3′ | 58 | 35 |
| | Reverse | 5′-ATGGGAGTTGGGCAGTCATCAG-3′ | | |
| iNOS | Forward | 5′-CTCCATGACTCTCAGCACAGAG-3′ | 58 | 30 |
| | Reverse | 5′-GCACCGAAGATATCCTCATGAT-3′ | | |
| MCP-1 | Forward | 5′-TCAGCCAGATGCAGTTAACG-3′ | 55 | 30 |
| | Reverse | 5′-GATCCTCTTGTAGCTCTCCAGC-3′ | | |
| MIP-1β | Forward | 5′-TCCCACTTCCTGCTGTTTCTCT-3′ | 60 | 34 |
| | Reverse | 5′-GAATACCACAGCTGGCTTGGA-3′ | | |
| Gro-α | Forward | 5′-CCGAAGTCATAGCCACACTCAA-3′ | 65 | 35 |
| | Reverse | 5′-GCAGTCGTCTCTTTCTCCGTTAC-3′ | | |
| MIP-2α | Forward | 5′-AGACAGAAGTCATAGCCACTCTCAAG-3′ | 62 | 35 |
| | Reverse | 5′-CCTCCTTTCCAGGTCAGTTAGC-3′ | | |
| GAPDH | Forward | 5′-AACTTTGGCATTGTGGAAGG-3′ | 50 | 23 |
| | Reverse | 5′-GGAGACAACCAGGTCCTCAG′ | | |

### 2.13. Axon staining and counting

After behavioral test, the rats from vehicle and PCA-treated groups were perfused at 38 d after injury, and frozen sections were prepared as described above. For quantitative analysis of axonal density, serial coronal sections collected every millimeter rostral and caudal 5 mm to the lesion site were stained with an antibody specific for 200 kDa neurofilament protein (NF200; 1:4,000, Sigma). Axonal densities were determined within preselected fields (40 × 40 μm, 1600 $\mu m^2$) at specific sites within the ventral and dorsolateral funiculi as previously described (Yune et al., 2007).

### 2.14. Assessment of lesion volume

The measurement of lesion volume using rats tested for behavioral analyses was performed as previously described (Yune et al., 2008). Serial longitudinal sections (10 μm) through the dorsoventral axis of the spinal cord were used to measure the volume of the lesion. Every 50 μm section was stained with Cresyl violet acetate. The rostrocaudal boundaries of the tissue damage were defined by the presence of inflammatory cells, the loss of neurons, the existence of degenerating neurons and cyst formation. The lesion area was determined by measuring the area of cavitation at the injury epicenter using a low-power (1.25×) objective and then calculated by means of a MetaMorph software (Molecular devices). Areas of each longitudinal level are determined, and the total lesion volume was induced by numerical integration of sequential areas.

### 2.15. Statistical analysis

All data are presented as the mean ± SD values, while hemorrhage, Evans blue, and BBB data are presented as the mean ± SEM. Comparisons between vehicle and PCA treated groups were made by unpaired Student's t-test. Multiple comparisons between groups were performed one-way ANOVA. Behavioral scores from BBB analysis were analyzed by repeated measured ANOVA (time vs treatment). Tukey's multiple comparison was used as Post hoc analysis. Statistical significance was accepted with $p < 0.05$. All statistical analyses were performed by SPSS 15.0 (SPSS Science, Chicago, IL).

## 3. Results

### 3.1. PCA inhibits apoptotic cell death of neurons and oligodendrocytes after SCI

It has been known that apoptotic cell death of neurons and oligodendrocytes at early and delayed stage after SCI contributes to the progressive degeneration of the spinal cord (Crowe et al., 1997; Liu and Luo, 1997). PCA is known to have neuroprotective effects in various neurological diseases such as AD and PD (Hornedo-Ortega et al., 2016; Zhang et al., 2015). Thus, based on our hypothesis that PCA might exhibit neuroprotective effect after SCI, we first examined the effect of PCA on the loss of VMN at 1 d after injury. As shown in Fig. 1A, a massive loss of VMN was observed in the lesion area as reported (Yune et al., 2008), while PCA treatment significantly alleviated VMN loss in both the rostral and caudal to the lesion epicenter when compared with vehicle-treated group (Fig. 1A and B). By TUNEL staining, TUNEL-positive cells were also observed mostly near and within the lesion site in the GM at 1 d after SCI. Most TUNEL-positive cells in the GM were demonstrated as neurons in our previous report (Lee et al., 2010). Furthermore, PCA treatment led to a significant reduction in the number of TUNEL-positive cells when compared to the vehicle-treated group (Fig. 1C and D) (Veh, 431 ± 31.7 vs. PCA, 262 ± 34.2, $p < 0.05$). In addition, PCA treatment significantly decreased the levels of cleaved forms of caspase-3 at 4 h after injury as compared to vehicle control (Fig. 1E) (Veh, 4.4 ± 0.3 vs. PCA, 3.2 ± 0.2, $p < 0.05$).

Next, we determined the effect of PCA on oligodendrocyte cell death at 5 d after injury. As in our previous reports (Lee et al., 2010; Yune et al., 2009), most TUNEL-positive cells were observed in the outside of the lesion area, extending the entire length of section (20 mm) in the WM, which were identified as oligodendrocytes (Fig. 2A). Quantitative analysis shows that PCA treatment significantly decreased the numbers of TUNEL-positive cells in the WM at 5 d, when compared to vehicle control (Fig. 2B) (Veh, 226 ± 15.4 vs. PCA, 131.5 ± 13.8, $p < 0.05$). Immunostaining with activated (cleaved) caspase-3 antibody also reveals that PCA treatment significantly reduced the number of activated caspase-3 positive cells in the WM at 5 d after injury as compared to vehicle control (Fig. 2C and D) (Veh, 211 ± 15 vs. PCA, 143 ± 17; $p < 0.05$). Double immunohistochemistry shows that cleaved caspase-3-positive cells in the WM at 5d after SCI were CC1-positive oligodendrocytes (Fig. 2D). Furthermore, Western blot and quantification analysis show that the level of cleaved caspase-3 was increased after SCI and its level was significantly decreased in the PCA-treated group as compared to vehicle control (Fig. 2E and F) (Veh, 4.6 ± 0.5 vs. PCA, 3.1 ± 0.2, $p < 0.05$). Thus, our results indicate that PCA inhibited apoptotic cell death of neurons and oligodendrocytes after injury.

### 3.2. PCA inhibits BSCB disruption and hemorrhage after SCI

It is well known that one of the earliest events ensuing traumatic SCI is the disruption of BSCB (Garcia et al., 2016), and blocking BSCB disruption attenuates the infiltration of blood cells causing inflammation, thereby improves functional recovery (Lee et al., 2012a, 2014). Thus, we evaluated the effect of PCA on BSCB disruption and hemorrhage at 1 d after injury using the Evans blue assay and intraspinal hemorrhage assay. As shown in Fig. 3A, the amount of Evans blue dye extravasation was increased after SCI when compared with the sham control, which indicates that BSCB disruption was induced after SCI. Furthermore, PCA treatment significantly reduced the amount of Evans blue dye extravasation when compared with the vehicle control, indicating PCA treatment attenuated BSCB disruption after SCI (Fig. 3B) (Veh, 54.9 ± 5.1 vs. PCA, 12.2 ± 1.9 μg/g tissue, $p < 0.05$). The hemorrhage assay also shows that the amount of intraspinal blood was increased after injury, but was significantly reduced by PCA treatment when compared with the vehicle control (Fig. 3C and D) (Veh, 2.22 ± 0.11 vs. PCA, 1.18 ± 0.15 μl, $p < 0.05$). These results indicate that PCA effectively prevented hemorrhage after SCI.

We next examined the effect of PCA on the loss of tight junction (TJ) proteins such as ZO-1 and occludin at 4 h and 5 d after injury. It is known that the TJ in the endothelial cells of the blood vessels maintains blood-brain barrier integrity (Zlokovic, 2008). The loss or degradation of TJ proteins has been implicated to mediate the hyperpermeability of BSCB after SCI (Lee et al., 2012a, 2012b). We previously showed that the antibodies against ZO-1 and occludin showed specific immunoreactivity at the expected molecular weights for the proteins (65 kDa for occludin, 220 kDa for ZO-1). The data show that the decrease in ZO-1 and occludin expression was especially prominent at 4 h and 5 d after injury respectively (Fig. 3E). Furthermore, the decrease of ZO-1 and occludin level was significantly attenuated in PCA-treated group compared to vehicle control (Fig. 3E and F) (ZO-1; Veh, 0.5 ± 0.03 vs. PCA, 0.8 ± 0.02, occludin; Veh, 0.2 ± 0.09 vs. PCA, 0.9 ± 0.07, $p < 0.05$), indicating that PCA treatment preserved TJ integrity by inhibiting TJ proteins loss after injury.

### 3.3. PCA inhibits the expression and activation of MMP-9 after SCI

Our recent reports showed that the excessive proteolytic activity of MMPs, such as MMP-2 and MMP-9, results in BSCB disruption after SCI (Lee et al., 2012a, 2012b). Because PCA treatment attenuated the BSCB disruption after SCI (Fig. 3), we investigated whether PCA would inhibit the expression and activity of MMP-2 and MMP-9 after injury. As

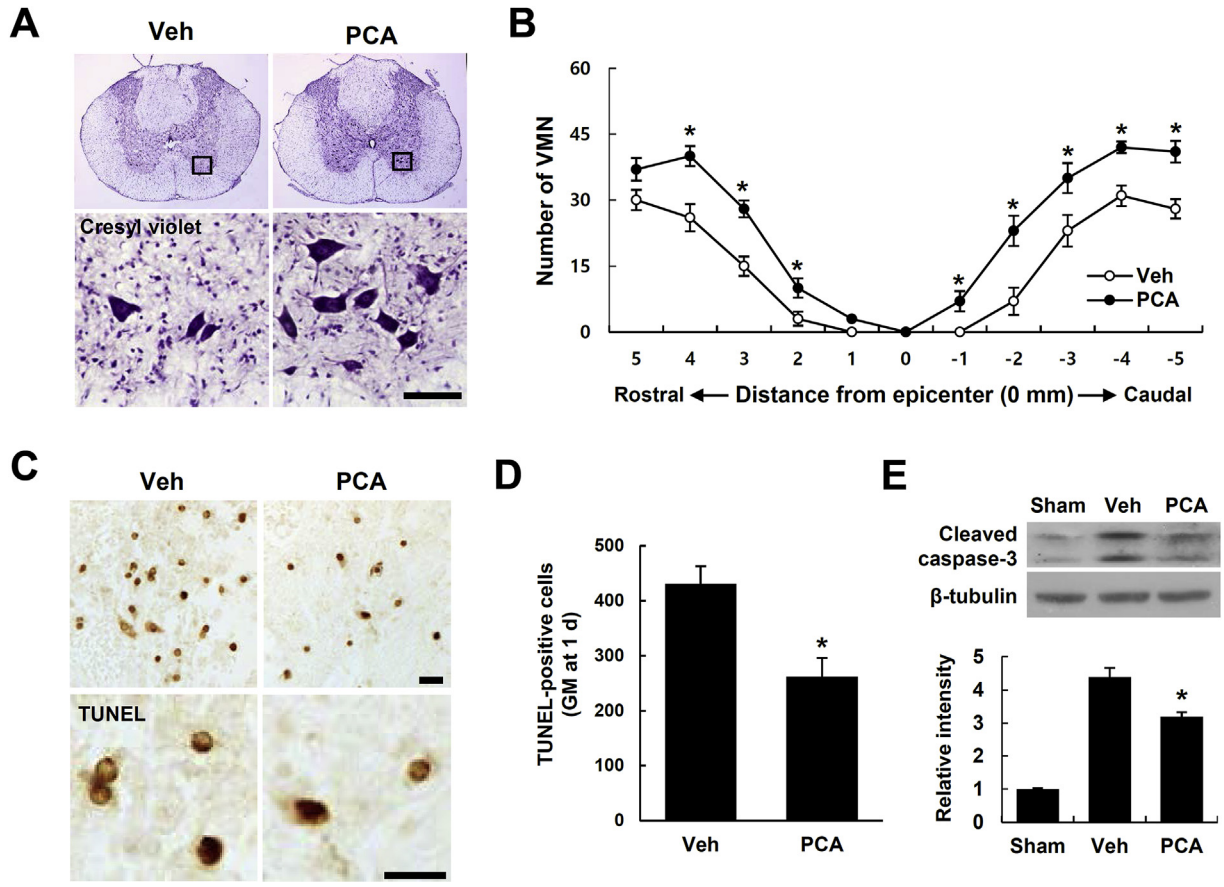


**Fig. 1.** Protocatechuic acid (PCA) inhibits apoptotic cell death of neurons after spinal cord injury (SCI). (A) Representative Cresyl violet staining showing ventral horn of spinal cord at 2 mm rostral from lesion site at 1 d. Scale bar, 50 μm. (B) Spatial pattern of the number of viable motor neurons (VMN). (C) Representative TUNEL staining showing the gray matter (GM) of spinal cord at 2 mm rostral form lesion site at 1 d. (D) Quantitative analysis of TUNEL-positive cells (n = 5). Scale bars, 20 μm. (E) Western blot of cleaved caspase-3 at 4 h after injury and densitometric analysis of Western blots (n = 3). All data represent mean ± SD. *$p < 0.05$ vs. vehicle.

shown in Fig. 4A and B, the levels of *Mmp-2* and *Mmp*-9 mRNA were increased after injury compared with the sham control. However, SCI-induced increase in *Mmp*-9 mRNA expression was significantly inhibited by PCA treatment at 6 h and 1 d after injury compared with the vehicle control, while *Mmp*-2 mRNA expression appeared to be unaffected by PCA (Fig. 4A and B). Using gelatin zymography, the increase of MMP-9 activity was also observed at 1 d after SCI (Fig. 4C), but the active MMP-2 band was not changed as in previous reports. Furthermore, the increase in MMP-9 activity after SCI was significantly inhibited by PCA compared with the vehicle control (Fig. 4D) (MMP-9; Veh, 8.9 ± 0.4 vs. PCA, 4.9 ± 0.7, $p < 0.05$).

### 3.4. PCA inhibits SUR1 and TrpM4 expression after SCI

It is known that both SUR1 and TrpM4 are up-regulated in the endothelial cells of blood vessels after SCI and mediate progressive hemorrhagic necrosis (Gerzanich et al., 2009; Simard et al., 2007). To investigate whether PCA would inhibit SCI-induced hemorrhage, we examined the effect of PCA on SUR1/TrpM4 expression using RT-PCR and Western blot analysis at 2 h, 6 h, and 1 d after injury. As shown in Fig. 5A, the mRNA expression of *Abcc8* was increased at 2 h and 6 h after injury, which was significantly inhibited by PCA treatment. In addition, the mRNA expression of *Trpm4* was increased at 2 h, 6 h, and 1 d after SCI, and PCA significantly reduced the mRNA level of *Trpm4* at 2 h, 6 h and 1 d after injury (Fig. 5A). Furthermore, the protein levels of SUR1 at 1 h and TrpM4 at 8 h after injury were also reduced by PCA treatment as compared with the vehicle control (Fig. 5B) (SUR1; Veh, 1.1 ± 0.04 vs. PCA, 0.7 ± 0.07, TrpM4; Veh, 1.0 ± 0.08 vs. PCA, 0.6 ± 0.03, $p < 0.05$).

### 3.5. The infiltration of neutrophils and macrophages is blocked by PCA after SCI

The infiltration of blood cells such as neutrophils and macrophages is followed by BSCB disruption and hemorrhage after SCI (Mun-Bryce and Rosenberg, 1998). Since PCA prevented BSCB disruption and hemorrhage after SCI, we examined the effect of PCA treatment on the infiltration of blood cells by immunohistochemistry using the antibodies against MPO and ED-1 respectively, and Western blot analysis for ED-1. As shown in Fig. 6A, both MPO-positive neutrophils at 1 d and ED-1-positive macrophages at 5 d after injury were mainly observed in the dorsal funiculus of injured spinal cord. The relative fluorescence intensity analysis shows that PCA treatment significantly inhibited the infiltration of neutrophils and macrophages compared with the vehicle control (Fig. 6A and B) (MPO: Veh, 1.0 ± 0.09 vs. PCA, 0.5 ± 0.05; ED-1: Veh, 1.0 ± 0.05 vs. PCA, 0.6 ± 0.04, $p < 0.05$). The Western blot analysis also reveals that the SCI-induced increase of the ED-1 level in the injured spinal cord lysates at 5 d after injury was significantly reduced by PCA treatment compared with the vehicle control (Fig. 6C) (Veh, 1.0 ± 0.04 vs. PCA, 0.5 ± 0.07, $p < 0.05$). These findings suggest that PCA inhibited blood cell infiltration by preventing BSCB disruption and hemorrhage after SCI.

### 3.6. PCA inhibits the expression of inflammatory mediators after SCI

After SCI, BSCB disruption followed blood cell infiltration is known

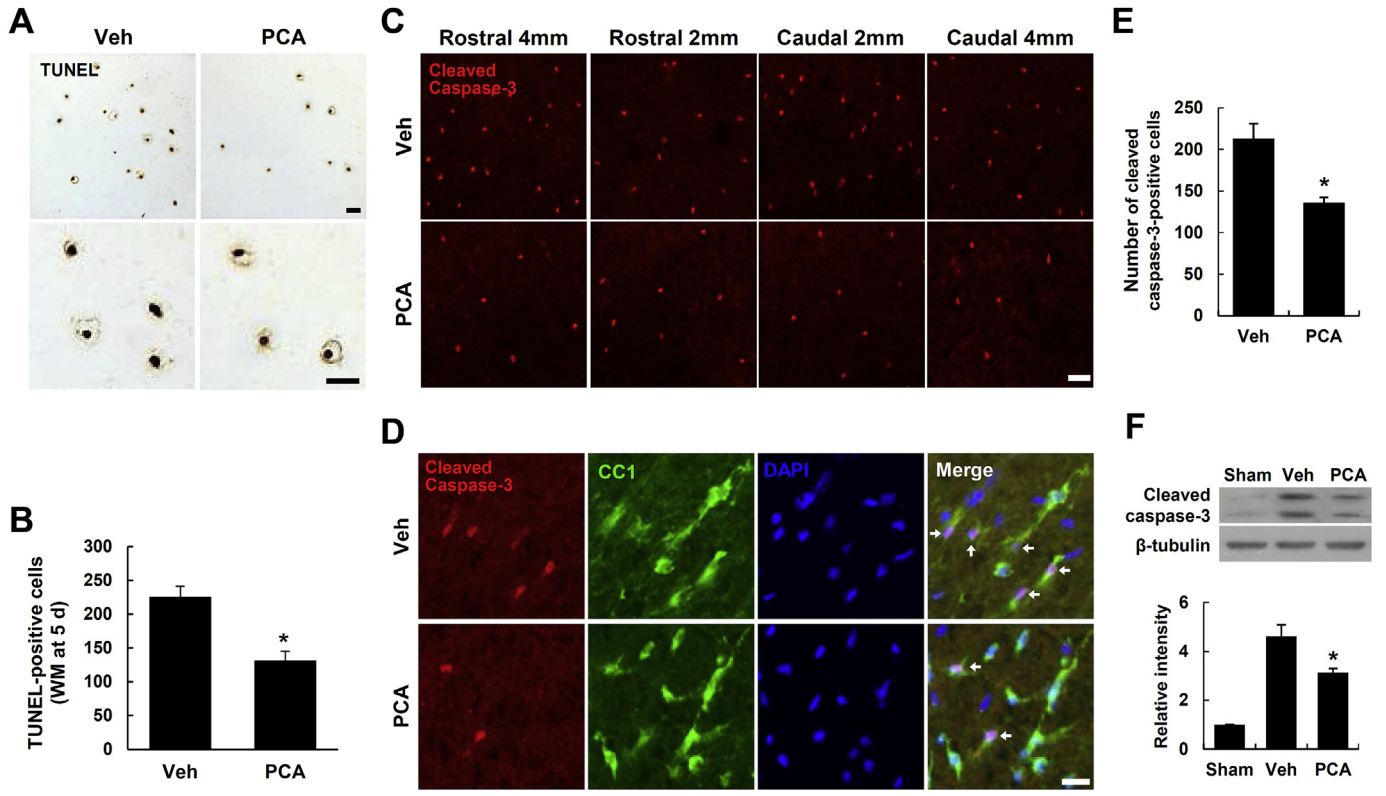


**Fig. 2.** PCA inhibits oligodendrocyte cell death after SCI. (A) Representative images of TUNEL staining at 5 d after SCI in the white matter (WM). Bottom panels show high-power views. Representative images are from sections 5 mm rostral to the lesion epicenter. Scale bars, 20 μm. (B) Quantitative analysis of TUNEL-positive cells. (C) Immunostaining of cleaved caspase-3 in the WM at 5 d after injury (n = 3). Scale bar, 20 μm. (D) Double labeling of cleaved caspase-3 and CC1-positive oligodendrocytes in the WM at 5 d after SCI. Spinal cord labeled with caspase-3 in red, CC1 in green, and DAPI in blue. Scale bar, 30 μm. (E) Quantitative analysis of cleaved caspase-3 positive cells with sections 4 mm rostral to the lesion epicenter. Data represent mean ± SD. $^*p < 0.05$ vs. vehicle. (F) Western blot of cleaved caspase-3 and densitometric analysis of Western blots (n = 3). Data are presented as means ± SD. $^*p < 0.05$ vs. vehicle.

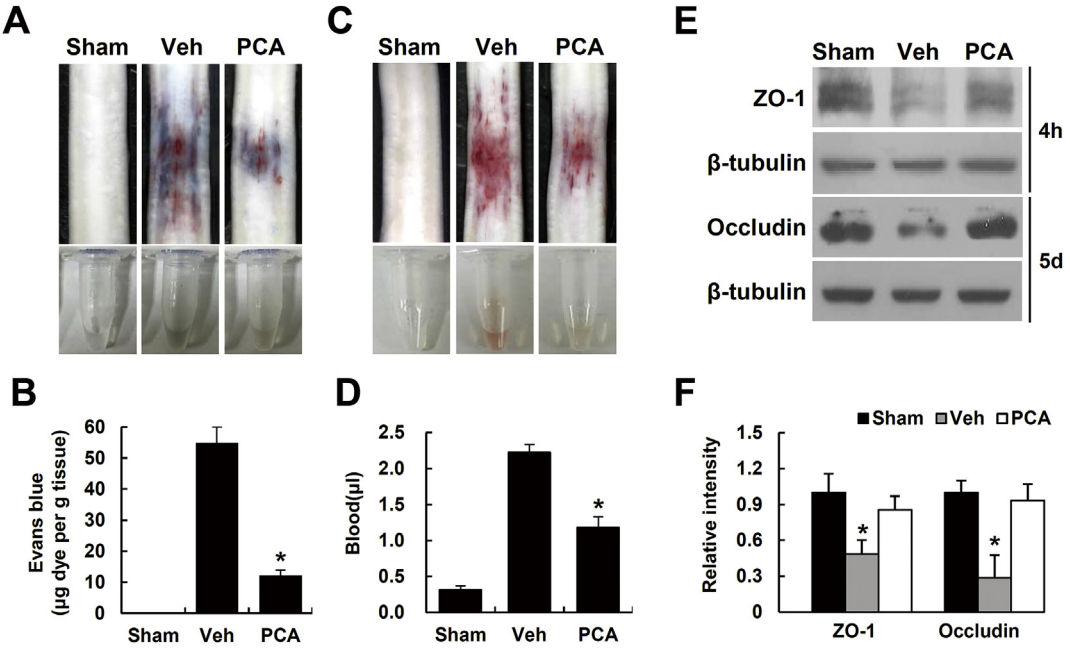


**Fig. 3.** PCA alleviates BSCB disruption and hemorrhage after SCI. For measurement of the BSCB permeability, 5 ml of 2% Evans blue dye was administered i.p. at 1 d after SCI and 3 h later, spinal tissues were prepared for detection and quantification of Evans blue extravasation. (A) Representative whole spinal cords showing Evans blue dye permeabilized into the spinal cord at 1 d. (B) Quantification of the Evans blue extravasation by using fluorometer (excitation at 620 nm and emission at 680 nm) (n = 3). The value was presented as an amount of dye (μg)/tissue weight (g). Data represent as mean ± SEM. $^*p < 0.05$ vs. vehicle. (C) Representative whole spinal cords and spinal cord homogenates in e-tube. (D) Spectrophotometric quantification of the amount of blood in homogenates from vehicle and PCA-treated rats (n = 5). Data represent mean ± SEM. $^*p < 0.05$ vs. vehicle. (E) Western blots of ZO-1 and occludin at 4 h and 5 d after injury respectively. (F) Densitometric analyses of Western blot (n = 3). Data represent mean ± SD. $^*p < 0.05$ vs. vehicle.

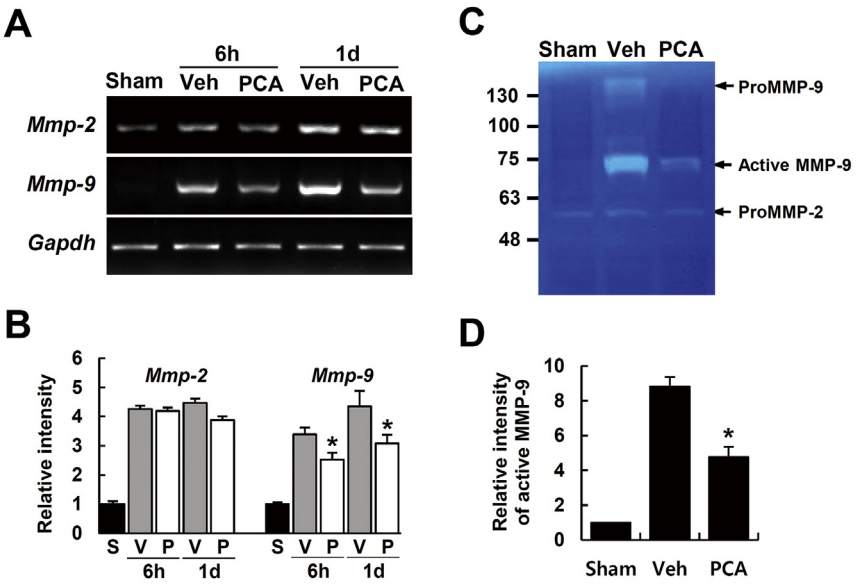


**Fig. 4.** PCA inhibits MMP-9 expression and activation after SCI. Rat was administrated immediately with PCA (50 mg/kg) after SCI and spinal cord tissues were isolated at 6 h and 1 d after injury. RT-PCR and gelatin zymography were processed as described in the Materials & methods section. (A) RT-PCR for *Mmp*-2 and *Mmp*-9 at 6 h and 1 d after SCI. (B) Densitometric analysis of RT-PCR (n = 3). (C) Gelatin zymography at 1 d after injury. (D) Densitometric analysis of zymography (n = 3). Note that PCA treatment significantly inhibits MMP-9 expression and activation after SCI. All data represent mean ± SD. *$p < 0.05$ vs. vehicle.

to mediate inflammation, thereby contributes to the secondary injury cascade by producing inflammatory mediators such as interleukin 1 beta (*Il-1β), tumor necrosis factor alpha (Tnf-α), Cox-2*, and *iNos* (Lee et al., 2012a, 2012b; Mun-Bryce and Rosenberg, 1998). In addition, the early increase of chemokines such as monocyte chemoattractant protein 1 (*Mcp-1),* macrophage inflammatory protein 1 beta *(Mip-1β),* growth regulated oncogene alpha (*Gro-α*) and macrophage inflammatory protein 2 alpha (*Mip-2α*) after SCI is known to induce the infiltration of neutrophils and macrophages, thereby facilitates inflammatory responses (Ghirnikar et al., 2001; McTigue et al., 1998; Ousman and David, 2001; Pineau and Lacroix, 2007). Thus, we next determined the effect of PCA on the expression of inflammatory mediators and chemokines after SCI by RT-PCR and Western blot. The results show that the increase of *Tnf-α*, *IL-1β* (at 2 h), *Cox-2* and *iNos* (at 6 h) mRNA level after SCI was significantly inhibited by PCA (Fig. 7A and B). In addition, PCA significantly inhibited the increases in the mRNA levels of *Mcp-1, Mip-1β, Gro-α* (at 2 h) and *Mip-2α* (at 8 h) after injury (Fig. 7C and D). The protein levels of iNOS and COX-2 at 1 d after injury were also significantly reduced by PCA as compared with the vehicle control (Fig. 7E and F).

### 3.7. PCA improves functional recovery after SCI

To determine the effect of PCA on functional recovery, we injected PCA (50 mg/kg) intraperitoneally at immediate, 2 h, and 6 h after injury and then further treated once a day for 7 d. Functional recovery was evaluated for 35 d after injury using the BBB rating scale, inclined plane test, grid walk test, and foot print analysis. As shown in Fig. 8A, PCA significantly increased the hindlimb locomotor function from 14 d to 35 d after injury as compared with the vehicle-treated group (At 35 d, PCA 13.2 ± 0.4 vs. Veh 9.0 ± 0.3, $p < 0.05$). In addition, the ability to control and place the hindlimbs precisely was examined on a horizontal grid at 35 d after injury. As shown in Fig. 8B, the number of mistakes (footfalls on the grid walk) in the PCA-treated group was significantly lower than that observed in the vehicle group (PCA 46.6 ± 6.1 vs. Veh 80 ± 6.3, $p < 0.05$). The angle of incline determined for 28 d after injury was also significantly higher in PCA-treated rat from 14 d to 28 d than in the vehicle group (Fig. 8C) (At 4 weeks, PCA 72.08 ± 2.1 vs. Veh 58.43 ± 1.8%, $p < 0.05$). Finally, footprint analysis shows that fairly consistent forelimb-hindlimb coordination was observed in both vehicle-treated and PCA-treated rats at

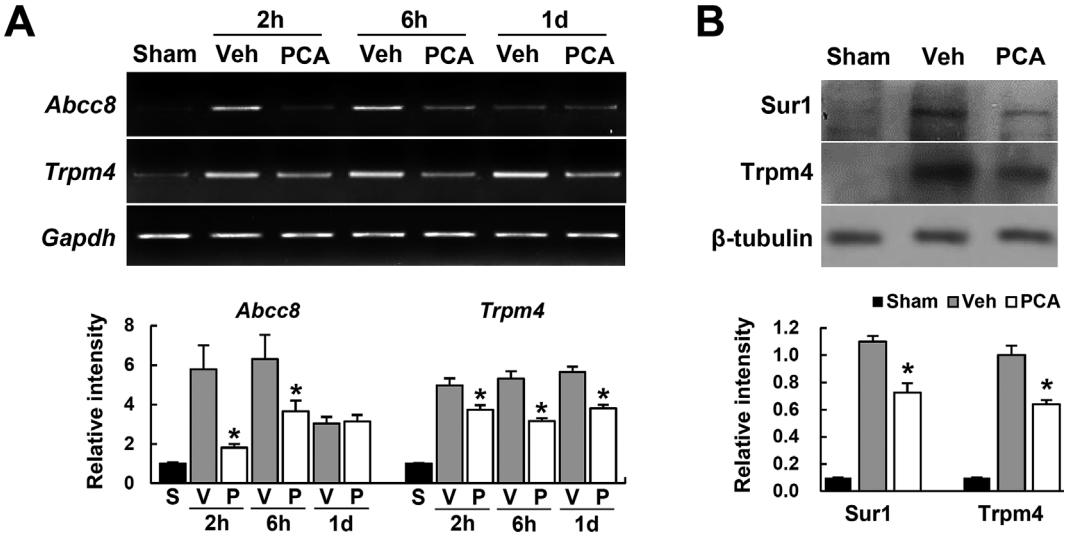


**Fig. 5.** PCA inhibits the expression of SUR1/TrpM4 after SCI. (A) RT-PCR (upper) and densitometry analysis (bottom) for *Abcc8* and *TrpM4* at 2 h, 6 h, and 1 d after SCI (n = 3). (B) Western blot (upper) and densitometric analyses (bottom) of SUR1 at 1 h and TrpM4 protein at 8 h after SCI (n = 3). Data represent mean ± SD. *$p < 0.05$ vs. vehicle.

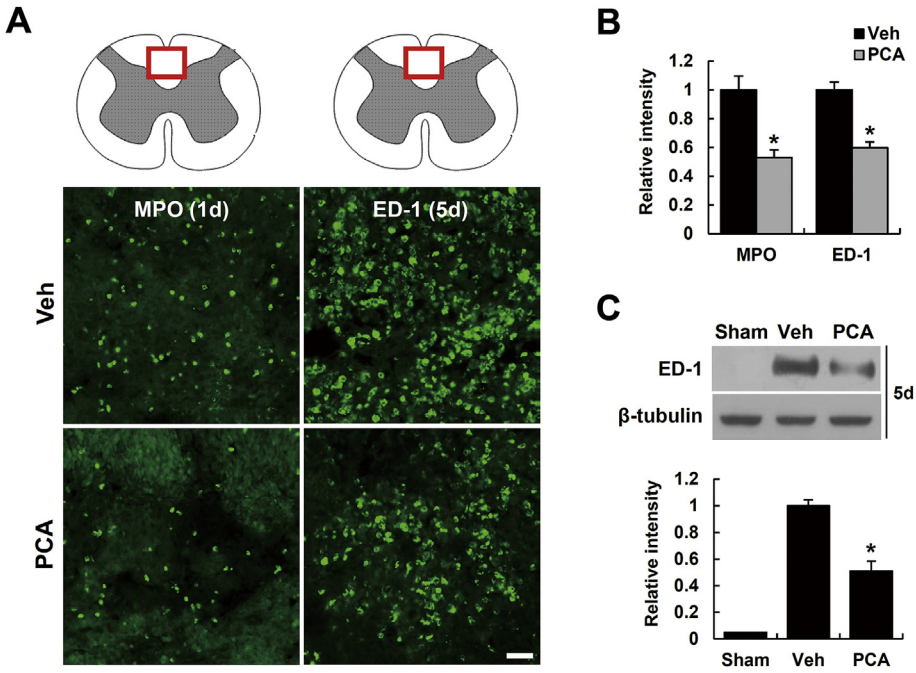


**Fig. 6.** PCA attenuates neutrophils and macrophages infiltration after SCI. After SCI, blood infiltration was assessed by measuring the fluorescent intensity of MPO or ED-1 immunoreactive area at 1 and 5 d or Western blot for ED-1 at 5 d after injury as described in the Materials & methods section. (A) Representative photographs at 2000 μm caudal to lesion epicenter showed MPO-labeled neutrophils or ED-1-labeled macrophages in the dorsal column of injured spinal tissues (cross section) injected with and without PCA. Scale bar, 50 μm. (B) Relative fluorescent intensity of MPO- and ED-1-positive cells (n = 3). (C) Western blot (upper) and densitometric analysis (bottom) of ED-1 at 5 d after injury. Note that PCA treatment significantly inhibited the infiltration of blood cells after SCI when compared to vehicle control. All data represent mean ± SD. *$p < 0.05$ vs. vehicle.

35 d after SCI, but very little toe dragging was shown in the PCA-treated group, in contrast to inconsistent dorsal stepping and extensive drags in the vehicle rats, as revealed by ink streaks extending from both hindlimbs (Fig. 8D).

### 3.8. PCA alleviates axon and myelin loss and decreases lesion volume after SCI

To confirm the correlation between behavioral data and histological findings such as axon loss, myelin loss and lesion volume, we performed histological analysis with the spinal cord tissues used for behavioral experiments. To examine whether PCA would preserve axons after injury, immunostaining with NF200 and 5-HT antibodies was performed to detect the remaining axons, and the density of preserved axons was measured as described in Materials and Methods. In sham control, NF200-positive axons in both ventral and dorsolateral funiculi were dense, and axonal packing was uniform (Fig. 9A and B, Sham). However, the axon density was markedly decreased in injured tissue (Fig. 9A and B, Veh). The number of NF200 positive axons in both ventral and dorsolateral funiculi were significantly higher in the PCA-treated group than in the vehicle-treated group (Fig. 9A and B) (rostral 2 mm, dorsolateral funiculus, PCA 66 ± 3.3 vs. Veh 36 ± 2.4%; ventral funiculus, PCA 68 ± 2.7 vs. Veh 33 ± 2.6%, $P < 0.05$). Moreover, the density of 5-HT serotonergic axons in the ventral horn was higher in the PCA-treated group than in the vehicle-treated group (Fig. 9C). These results indicate that PCA treatment alleviated axon loss after SCI.

Next, the extent of myelin loss after injury was assessed by Luxol fast blue staining. As shown in Fig. 9D, extensive myelin loss near the lesion area was evident in the vehicle-treated group at 38 d after injury compared with the sham control (Fig. 9D, Veh), whereas PCA treatment apparently attenuated myelin loss (Fig. 9D, PCA). To evaluate tissue loss after SCI, serial longitudinal sections were stained with Cresyl violet and lesion volume was measured. As shown in Fig. 9E, total lesion volume was significantly reduced in PCA-treated group at 38 d after injury as compared to the vehicle-treated group (Fig. 9E) (PCA, 5.2 ± 0.5 vs. Veh, 9.2 ± 1.4 $mm^3$, $P < 0.05$).

## 4. Discussion

In this study, we demonstrated that PCA has neuroprotective effects by preventing BSCB disruption and hemorrhage via inhibiting MMP-9 activation and SUR1/TrpM4 expression after SCI. PCA also alleviated the infiltration of blood cells such neutrophils and macrophages after injury, thereby inhibited the expression of inflammatory factors such as TNF-α, IL-1β, COX-2, iNOS and chemokines such as *Mcp-1, Mip-1β, Gro-α*, and *Mip-2α*, resulting in reduced inflammatory responses. Furthermore, PCA treatment inhibited apoptotic cell death of neurons and oligodendrocytes and improved functional recovery after SCI. Thus, our study suggests the neuroprotective effect of PCA was in part mediated by inhibiting BSCB disruption and hemorrhage after SCI. In our knowledge, this is the first report that shows the effectiveness of the PCA on BSCB disruption and hemorrhage. However, our present study did not examine whether the effect of PCA on axon loss, BSCB disruption and apoptotic cell death would be mediated directly or indirectly. Therefore, the precise neuroprotective mechanism of PCA, and whether the effect of PCA would be directly targeted on neurons, oligodendrocytes and endothelial cell after SCI will be investigated as a future study.

PCA has been recognized as a cytoprotective agent through its anti-apoptotic, anti-oxidative, and anti-inflammatory effects in previous studies (Masella et al., 2012; Tsao et al., 2014; Yin et al., 2015). Recent studies also reported the neuroprotective effect of PCA in CNS disease animal models. In a pilocarpine induced rat seizure model, PCA (30 mg/kg, i.p.) treatment reduced neuronal cell death and inhibited microglia activation in hippocampus (Lee et al., 2018b). The report by Lee et al. (2017) also showed that daily injection of PCA (30 mg/kg, i.p.) for 7 d significantly inhibits neuronal cell death in the hippocampus and cortex and alleviates oxidative stress after traumatic brain injury. In this study, PCA was administered via i.p. injection at a dose of 50 mg/kg immediately after SCI and then injected the same dose of PCA at 6 h and 12 h after injury, and then further treated once a day for 7 d. When we tested the efficacy of various concentrations of PCA (20, 50, 100, 200 mg/kg), 50 mg/kg of PCA was most effective for functional recovery after SCI (See Supplementary Fig. 1). Therefore, we determined that 50 mg/kg was the optimal concentration of PCA in this study and any significant change in body weight among the experimental groups during our experiment was not observed (Fig. 8E). In addition, neither significant side effect nor increasing of mortality by PCA treatment was also observed.

After SCI, vascular events of secondary damage including

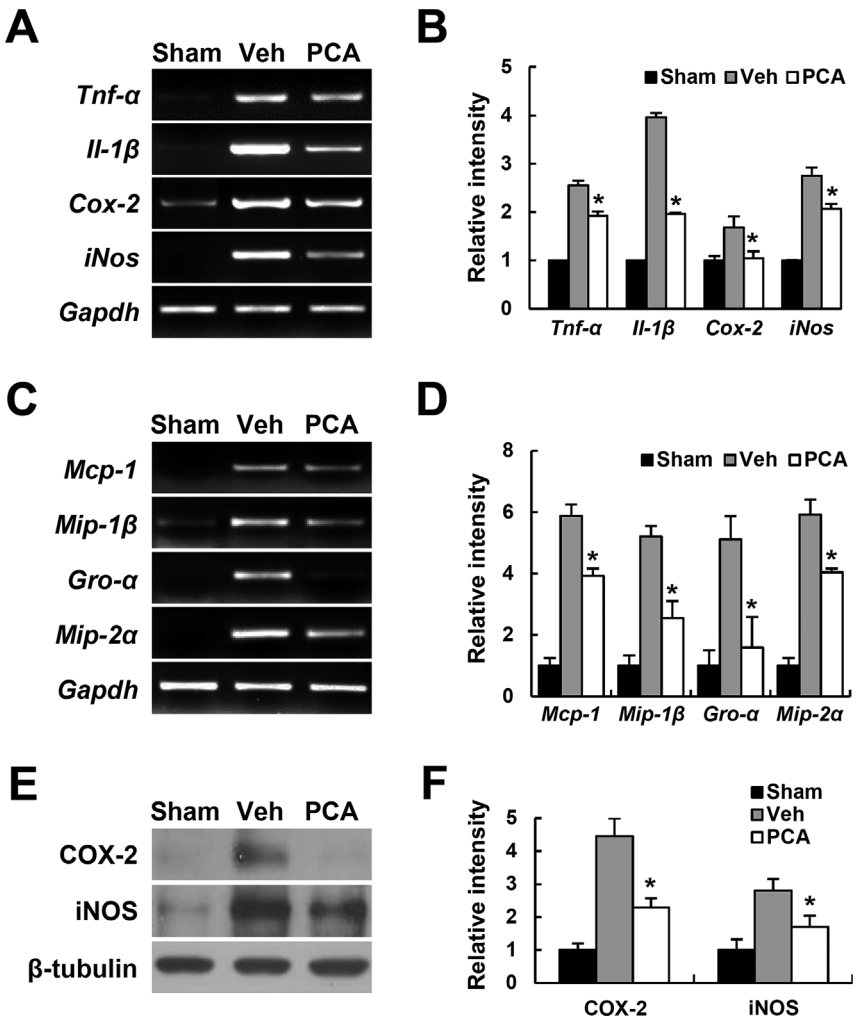


**Fig. 7.** PCA inhibits the expression of inflammatory factors after SCI. Total RNA and protein extracts from vehicle or PCA-treated spinal cords at indicated time points after injury were prepared. (A) RT-PCR of *Il-1β* and *Tnf-α* (at 2 h), *Cox-2* and *iNos* (at 6 h) after injury. (B) Quantitative analyses of RT-PCR (n = 3). (C) RT-PCR of *MCP-1*, *MIP-1β* and *MIP-2α* (at 2 h), *Gro-α* (at 6 h) after injury (n = 3). (D) Quantitative analyses of RT-PCR (n = 3). (E) Western blots of iNOS and COX-2 at 1 d after injury. (F) Quantification analysis of Western blot (n = 3). Data represent mean ± SD. *$p < 0.05$ vs. vehicle.

hemorrhage and BSCB disruption are observed. It is generally known that the up-regulation of MMP-9 is closely associated with BSCB breakdown by degrading the basal component of BSCB such as TJ proteins. The BSCB breakdown also facilitates immune cells infiltration and triggers the post-traumatic inflammatory response (Hausmann, 2003; Lee et al., 2015a; Noble et al., 2002). Our data showed that MMP-9 expression and gelatinase activity are significantly inhibited by PCA treatment (see Fig. 4). TJ proteins, occludin and ZO-1 were also degraded after SCI and PCA treatment significantly preserved these molecules (see Fig. 3E). In addition, blood-brain barrier disruption was attenuated in MMP-9 knockout mice after cerebral ischemia by reducing the degradation of ZO-1 protein as compared with wild type mice (Asahi et al., 2001). Furthermore, recent reports provided the evidence that BSCB disruption is significantly reduced when the expression and activation of MMP-9 are inhibited (Lee et al., 2012a, 2014, 2018a). Thus, these results indicate that PCA prevented BSCB disruption by inhibiting MMP-9 expression and activity after SCI. However, it is now yet known how PCA inhibits MMP-9 expression after SCI. We recently found that histone H3K27 demethylase, Jmjd3, plays as a critical epigenetic regulator in MMP-9 expression in vascular endothelial cells after SCI (Lee et al., 2016). As a preliminary study, we also found that PCA treatment significantly blocks Jmjd3 expression at 2 h and 8 h after injury (data not shown). Thus, our preliminary result suggests the possibility that PCA may inhibit MMP-9 expression through the regulation of Jmjd3 expression. The precise mechanism underlying PCA-mediated inhibition of MMP-9 expression after SCI will be investigated in the future study.

After contusive SCI, a small bleeding lesion appeared near the injury epicenter within 15 min after initial injury, and then petechial hemorrhage is observed in distant area resulting in progressive hemorrhagic necrosis (Gerzanich et al., 2009). It was reported that SUR1 and TrpM4 expression are increased in the capillary endothelium and is closely involved in the molecular mechanisms underlying progressive hemorrhagic necrosis after SCI (Lee et al., 2015a). Several reports showed that the uncontrolled activation of SUR1-regulated TrpM4 channel after injury results in oncotic death of CNS endothelium, leading to ischemia and disintegration of neural tissue (Gerzanich et al., 2009; Simard et al., 2007, 2010). Thus, these channels could be therapeutically targeted in traumatic neurological disorders. Consistent with this suggestion, an anti-diabetic drug, glibenclamide, a potent blocker of SUR1-regulated TrpM4 channel, has been shown to reduce edema and the loss of neural tissue and to improve functional outcome in diverse forms of CNS injuries such as SCI, TBI, and ischemic stroke (Gerzanich et al., 2009; Simard et al., 2007, 2010). Furthermore, we observed that the inhibition of SUR1/TrpM4 expression by ghrelin, 17-β estradiol, or mithramycin A significantly reduced SCI-induced hemorrhage and improved functional recovery after SCI (Lee et al., 2014, 2018a, 2015a). In this study, PCA treatment significantly reduced the up-regulation of

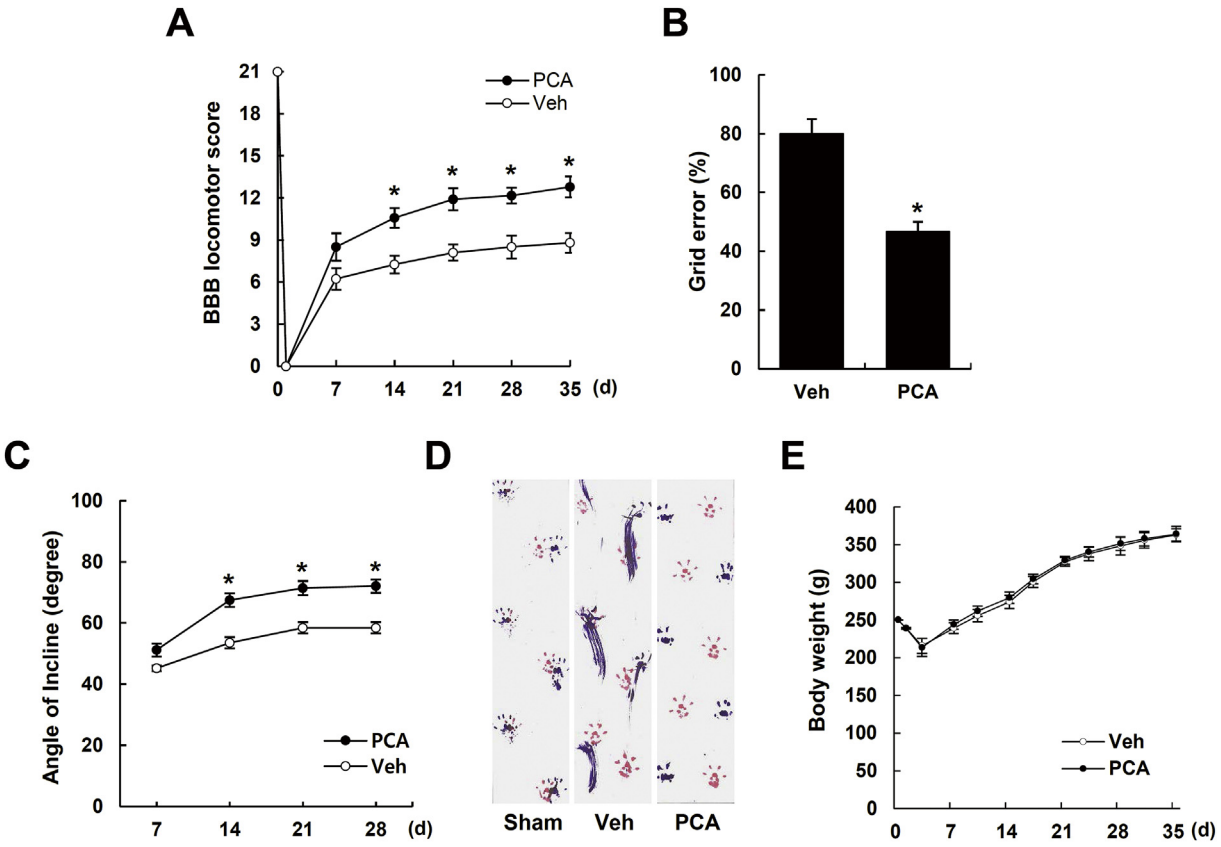


**Fig. 8.** PCA improves functional recovery after SCI. (A) BBB scores of vehicle and PCA-treated groups after injury. (B) Grid walk test of vehicle and PCA-treated groups at 35 d after injury. (C) Inclined plane test of vehicle- and PCA-treated groups after injury. (D) Representative footprints obtained from each group at 35 d after SCI. All data are presented as means ± SEM (n = 10). (E) Body weight. *$p < 0.05$ vs. vehicle.

both SUR1 and TrpM4 in mRNA and protein levels after SCI. These findings suggest that PCA treatment significantly attenuated hemorrhage after SCI by inhibiting the up-regulation of SUR1 and TrpM4 expression.

Inflammation is known as a critical event in the secondary damage after SCI. BSCB disruption and hemorrhage after injury lead to blood immune cells infiltration into the spinal cord parenchyma. The infiltrated immune cells produce inflammatory factors, thereby increase tissue damage, induce cell death, and impair locomotor behavior after SCI (Beattie et al., 2002; Carlson et al., 1998; Okada et al., 2004). Several studies also demonstrated that the suppression of neutrophils and macrophages infiltration after injury ameliorates apoptotic cell death and improves functional recovery (Saiwai et al., 2010; Taoka et al., 1997). Our study also showed that PCA treatment significantly inhibited the expression of inflammatory mediators (*iNos* and *Cox-2* at 1 d), cytokines (*TNF-α* and *Il-1β* at 2 h) and chemokines (*Mcp-1* and *Mip-2α* at 2 h; *Gro-α* and *Mip-1β* at 6 h) (see Fig. 7). Thus, our results suggest that the neuroprotective effect of PCA might in part by be inhibited the inflammatory response by protecting BSCB disruption followed the infiltration of neutrophils and macrophages after SCI. However, our present study did not show whether the anti-inflammatory effect of PCA would be mediated directly or indirectly after SCI. According to several studies, PCA was found to significantly inhibit the expression of inflammatory cytokines and inflammatory mediators such as IL-1β, TNF-α, COX-2 in LPS-induced macrophage (Min et al., 2010; Vari et al., 2015; Wei et al., 2012; Wu et al., 2016). These data suggest the possibility that PCA may exert its anti-inflammatory effect directly on immune cells after SCI. Additional studies are necessary to uncover the PCA-associated anti-inflammatory mechanisms after SCI. Recently, Lee et al. (2017) demonstrated that PCA preserves TBI-induced neuronal apoptosis in the hippocampus and cortex by inhibiting oxidative stress and restoration of neuronal glutathione, endogenous antioxidant enzyme. Since reactive oxygen species and oxidative stress have a significant role in the pathophysiology after SCI, we cannot rule out the possibility that PCA may exert a neuroprotective effect by inhibiting oxidative stress after SCI.

In summary, our findings showed that the neuroprotective effect of PCA is mediated, in part, by attenuating BSCB disruption and hemorrhage through the inhibition of the up-regulation of SUR1, TrpM4, and MMP-9 expression and the subsequent blood cells infiltration, thereby attenuating inflammatory responses after SCI. Thus, our study suggests that PCA may be potentially useful therapeutic agent for a traumatic SCI.

## Author disclosure statement

No competing financial interests exist.

## Acknowledgments

This research was supported by Basic Science Research Program through the National Research Foundation of Korea funded by the Ministry of Education (NRF-2016R1A6A3A11934000). This research was supported by the Korea Institute of Science and Technology Institutional Program (Project No. 2Z05460) and the Brain Research Program through the National Research Foundation of Korea funded by the Korean Government (MIST; 2017M37A1025369).

## Appendix A. Supplementary data

Supplementary data to this article can be found online at https://doi.org/10.1016/j.neuint.2019.01.013.

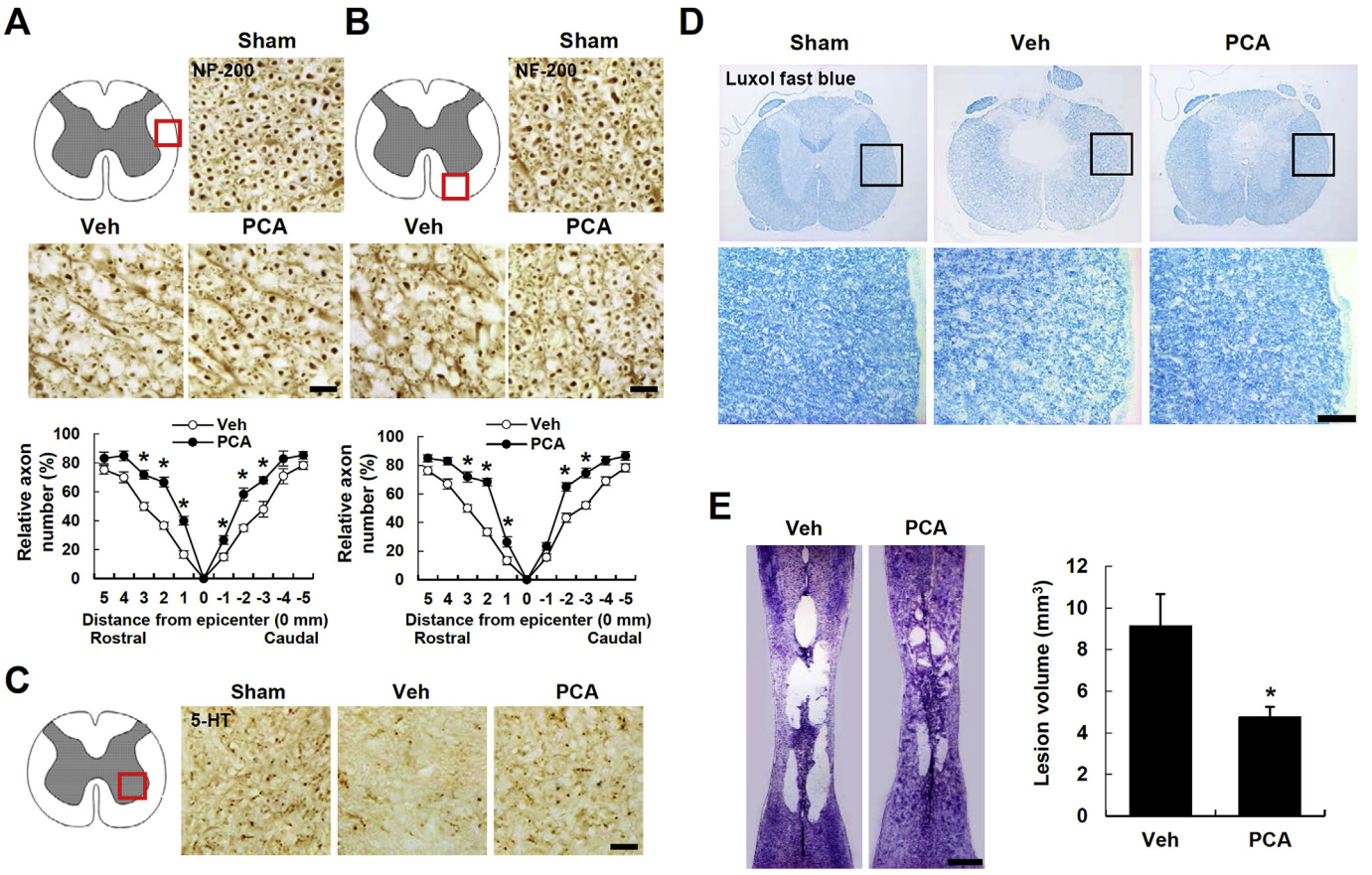


**Fig. 9.** PCA inhibits axon and myelin loss and reduces lesion volume after SCI. (A, B) Representative photographs of NF200-positive axons in spinal cords. Sections were selected 2 mm rostral to the lesion site. Note that PCA treatment decreased the extent of axon loss after injury. Scale bars, 20 μm. Quantitative analysis of NF200-positive axons in dorsolateral (A) and ventral (B) funiculi showed that the density of spared axons in the PCA-treated group was significantly higher than that in the vehicle control. NF200-positive axons were counted as described under Materials and Methods. (C) Representative photographs of 5-HT positive axons in ventral horn areas in sections 3 mm caudal to the lesion site. Scale bars, 30 μm. (D) Luxol fast blue staining shows that myelin loss in lateral funiculus after injury was extensive in the vehicle when compared with those in sham control. PCA treatment decreased the extent of myelin loss after injury. Scale bar, 100 μm. (E) Representative spinal cord tissues (1.2 mm from dorsal surface) showing the cavitation in the lesion site 38 d after injury.

## References


Abbott, N.J., Ronnback, L., Hansson, E., 2006. Astrocyte-endothelial interactions at the blood-brain barrier. Nat. Rev. Neurosci. 7, 41–53.

Asahi, M., Wang, X., Mori, T., Sumii, T., Jung, J.C., Moskowitz, M.A., Fini, M.E., Lo, E.H., 2001. Effects of matrix metalloproteinase-9 gene knock-out on the proteolysis of blood-brain barrier and white matter components after cerebral ischemia. J. Neurosci. 21, 7724–7732.

Basso, D.M., Beattie, M.S., Bresnahan, J.C., 1995. A sensitive and reliable locomotor rating scale for open field testing in rats. J. Neurotrauma 12, 1–21.

Beattie, M.S., Hermann, G.E., Rogers, R.C., Bresnahan, J.C., 2002. Cell death in models of spinal cord injury. Prog. Brain Res. 137, 37–47.

Carlson, S.L., Parrish, M.E., Springer, J.E., Doty, K., Dossett, L., 1998. Acute inflammatory response in spinal cord following impact injury. Exp. Neurol. 151, 77–88.

Crowe, M.J., Bresnahan, J.C., Shuman, S.L., Masters, J.N., Beattie, M.S., 1997. Apoptosis and delayed degeneration after spinal cord injury in rats and monkeys. Nat. Med. 3, 73–76.

Garcia, E., Aguilar-Cevallos, J., Silva-Garcia, R., Ibarra, A., 2016. Cytokine and growth factor Activation in vivo and in vitro after spinal cord injury. Mediat. Inflamm. 2016, 9476020.

Genovese, T., Esposito, E., Mazzon, E., Di Paola, R., Caminiti, R., Bramanti, P., Cappelani, A., Cuzzocrea, S., 2009. Absence of endogenous interleukin-10 enhances secondary inflammatory process after spinal cord compression injury in mice. J. Neurochem. 108, 1360–1372.

Gerzanich, V., Woo, S.K., Vennekens, R., Tsymbalyuk, O., Ivanova, S., Ivanov, A., Geng, Z., Chen, Z., Nilius, B., Flockerzi, V., Freichel, M., Simard, J.M., 2009. De novo expression of Trpm4 initiates secondary hemorrhage in spinal cord injury. Nat. Med. 15, 185–191.

Ghirnikar, R.S., Lee, Y.L., Eng, L.F., 2001. Chemokine antagonist infusion promotes axonal sparing after spinal cord contusion injury in rat. J. Neurosci. Res. 64, 582–589.

Guan, S., Jiang, B., Bao, Y.M., An, L.J., 2006. Protocatechuic acid suppresses MPP+-induced mitochondrial dysfunction and apoptotic cell death in PC12 cells. Food Chem. Toxicol. 44, 1659–1666.

Hausmann, O.N., 2003. Post-traumatic inflammation following spinal cord injury. Spinal Cord 41, 369–378.

Hawkins, B.T., Davis, T.P., 2005. The blood-brain barrier/neurovascular unit in health and disease. Pharmacol. Rev. 57, 173–185.

Hornedo-Ortega, R., Alvarez-Fernandez, M.A., Cerezo, A.B., Richard, T., Troncoso, A.M., Garcia-Parrilla, M.A., 2016. Protocatechuic acid: inhibition of fibril formation, destabilization of preformed fibrils of amyloid-beta and alpha-synuclein, and neuroprotection. J. Agric. Food Chem. 64, 7722–7732.

Keane, R.W., Davis, A.R., Dietrich, W.D., 2006. Inflammatory and apoptotic signaling after spinal cord injury. J. Neurotrauma 23, 335–344.

Lee, J.Y., Choi, H.Y., Na, W.H., Ju, B.G., Yune, T.Y., 2014. Ghrelin inhibits BSCB disruption/hemorrhage by attenuating MMP-9 and SUR1/TrpM4 expression and activation after spinal cord injury. Biochim. Biophys. Acta 1842, 2403–2412.

Lee, J.Y., Choi, H.Y., Na, W.H., Ju, B.G., Yune, T.Y., 2015a. 17 beta-estradiol inhibits MMP-9 and SUR1/TrpM4 expression and activation and thereby attenuates BSCB disruption/hemorrhage after spinal cord injury in male rats. Endocrinology 156, 1838–1850.

Lee, J.Y., Choi, H.Y., Park, C.S., Ju, B.G., Yune, T.Y., 2018a. Mithramycin a improves functional recovery by inhibiting BSCB disruption and hemorrhage after spinal cord injury. J. Neurotrauma 35, 508–520.

Lee, J.Y., Chung, H., Yoo, Y.S., Oh, Y.J., Oh, T.H., Park, S., Yune, T.Y., 2010. Inhibition of apoptotic cell death by ghrelin improves functional recovery after spinal cord injury. Endocrinology 151, 3815–3826.

Lee, J.Y., Kang, S.R., Yune, T.Y., 2015b. Fluoxetine prevents oligodendrocyte cell death by inhibiting microglia activation after spinal cord injury. J. Neurotrauma 32, 633–644.

Lee, J.Y., Kim, H.S., Choi, H.Y., Oh, T.H., Ju, B.G., Yune, T.Y., 2012a. Valproic acid attenuates blood-spinal cord barrier disruption by inhibiting matrix metalloprotease-9 activity and improves functional recovery after spinal cord injury. J. Neurochem. 121, 818–829.

Lee, J.Y., Kim, H.S., Choi, H.Y., Oh, T.H., Yune, T.Y., 2012b. Fluoxetine inhibits matrix metalloprotease activation and prevents disruption of blood-spinal cord barrier after spinal cord injury. Brain 135, 2375–2389.

Lee, J.Y., Na, W.H., Choi, H.Y., Lee, K.H., Ju, B.G., Yune, T.Y., 2016. Jmjd3 mediates

blood-spinal cord barrier disruption after spinal cord injury by regulating MMP-3 and MMP-9 expressions. Neurobiol. Dis. 95, 66–81.
Lee, S.H., Choi, B.Y., Kho, A.R., Jeong, J.H., Hong, D.K., Lee, S.H., Lee, S.Y., Lee, M.W., Song, H.K., Choi, H.C., Suh, S.W., 2018b. Protective effects of protocatechuic acid on seizure-induced neuronal death. Int. J. Mol. Sci. 19.
Lee, S.H., Choi, B.Y., Lee, S.H., Kho, A.R., Jeong, J.H., Hong, D.K., Suh, S.W., 2017. Administration of protocatechuic acid reduces traumatic brain injury-induced neuronal death. Int. J. Mol. Sci. 18.
Lin, H.H., Chen, J.H., Chou, F.P., Wang, C.J., 2011. Protocatechuic acid inhibits cancer cell metastasis involving the down-regulation of Ras/Akt/NF-kappaB pathway and MMP-2 production by targeting RhoB activation. Br. J. Pharmacol. 162, 237–254.
Liu, W., Luo, Y., 1997. Neurotrophic factors and spinal cord injury. A review. Zhongguo Xiu Fu Chong Jian Wai Ke Za Zhi 11, 19–21.
Masella, R., Santangelo, C., D'Archivio, M., Li Volti, G., Giovannini, C., Galvano, F., 2012. Protocatechuic acid and human disease prevention: biological activities and molecular mechanisms. Curr. Med. Chem. 19, 2901–2917.
McTigue, D.M., Tani, M., Krivacic, K., Chernosky, A., Kelner, G.S., Maciejewski, D., Maki, R., Ransohoff, R.M., Stokes, B.T., 1998. Selective chemokine mRNA accumulation in the rat spinal cord after contusion injury. J. Neurosci. Res. 53, 368–376.
Merkler, D., Metz, G.A., Raineteau, O., Dietz, V., Schwab, M.E., Fouad, K., 2001. Locomotor recovery in spinal cord-injured rats treated with an antibody neutralizing the myelin-associated neurite growth inhibitor Nogo-A. J. Neurosci. 21, 3665–3673.
Min, S.W., Ryu, S.N., Kim, D.H., 2010. Anti-inflammatory effects of black rice, cyanidin-3-O-beta-D-glycoside, and its metabolites, cyanidin and protocatechuic acid. Int. Immunopharm. 10, 959–966.
Mun-Bryce, S., Rosenberg, G.A., 1998. Gelatinase B modulates selective opening of the blood-brain barrier during inflammation. Am. J. Physiol. 274, R1203–R1211.
Noble, L.J., Donovan, F., Igarashi, T., Goussev, S., Werb, Z., 2002. Matrix metalloproteinases limit functional recovery after spinal cord injury by modulation of early vascular events. J. Neurosci. 22, 7526–7535.
Okada, S., Nakamura, M., Mikami, Y., Shimazaki, T., Mihara, M., Ohsugi, Y., Iwamoto, Y., Yoshizaki, K., Kishimoto, T., Toyama, Y., Okano, H., 2004. Blockade of interleukin-6 receptor suppresses reactive astrogliosis and ameliorates functional recovery in experimental spinal cord injury. J. Neurosci. Res. 76, 265–276.
Ousman, S.S., David, S., 2001. MIP-1 alpha, MCP-1, GM-CSF, and TNF-alpha control the immune cell response that mediates rapid phagocytosis of myelin from the adult mouse spinal cord. J. Neurosci. 21, 4649–4656.
Pineau, I., Lacroix, S., 2007. Proinflammatory cytokine synthesis in the injured mouse spinal cord: multiphasic expression pattern and identification of the cell types involved. J. Comp. Neurol. 500, 267–285.
Rivlin, A.S., Tator, C.H., 1977. Objective clinical assessment of motor function after experimental spinal cord injury in the rat. J. Neurosurg. 47, 577–581.
Saiwai, H., Ohkawa, Y., Yamada, H., Kumamaru, H., Harada, A., Okano, H., Yokomizo, T., Iwamoto, Y., Okada, S., 2010. The LTB4-BLT1 axis mediates neutrophil infiltration and secondary injury in experimental spinal cord injury. Am. J. Pathol. 176, 2352–2366.
Shi, G.F., An, L.J., Jiang, B., Guan, S., Bao, Y.M., 2006. Alpinia protocatechuic acid protects against oxidative damage in vitro and reduces oxidative stress in vivo. Neurosci. Lett. 403, 206–210.
Simard, J.M., Tsymbalyuk, O., Ivanov, A., Ivanova, S., Bhatta, S., Geng, Z., Woo, S.K., Gerzanich, V., 2007. Endothelial sulfonylurea receptor 1-regulated NC Ca-ATP channels mediate progressive hemorrhagic necrosis following spinal cord injury. J. Clin. Invest. 117, 2105–2113.
Simard, J.M., Woo, S.K., Norenberg, M.D., Tosun, C., Chen, Z., Ivanova, S., Tsymbalyuk, O., Bryan, J., Landsman, D., Gerzanich, V., 2010. Brief suppression of Abcc8 prevents autodestruction of spinal cord after trauma. Sci. Transl. Med. 2 28ra29.
Sinescu, C., Popa, F., Grigorean, V.T., Onose, G., Sandu, A.M., Popescu, M., Burnei, G., Strambu, V., Popa, C., 2010. Molecular basis of vascular events following spinal cord injury. J Med Life 3, 254–261.
Stirling, D.P., Khodarahmi, K., Liu, J., McPhail, L.T., McBride, C.B., Steeves, J.D., Ramer, M.S., Tetzlaff, W., 2004. Minocycline treatment reduces delayed oligodendrocyte death, attenuates axonal dieback, and improves functional outcome after spinal cord injury. J. Neurosci. 24, 2182–2190.
Taoka, Y., Okajima, K., Uchiba, M., Murakami, K., Kushimoto, S., Johno, M., Naruo, M., Okabe, H., Takatsuki, K., 1997. Role of neutrophils in spinal cord injury in the rat. Neuroscience 79, 1177–1182.
Thakare, V.N., Dhakane, V.D., Patel, B.M., 2017. Attenuation of acute restraint stress-induced depressive like behavior and hippocampal alterations with protocatechuic acid treatment in mice. Metab. Brain Dis. 32, 401–413.
Tsao, S.M., Hsia, T.C., Yin, M.C., 2014. Protocatechuic acid inhibits lung cancer cells by modulating FAK, MAPK, and NF-kappaB pathways. Nutr. Canc. 66, 1331–1341.
Vari, R., Scazzocchio, B., Santangelo, C., Filesi, C., Galvano, F., D'Archivio, M., Masella, R., Giovannini, C., 2015. Protocatechuic acid prevents oxLDL-induced apoptosis by activating JNK/Nrf2 survival signals in macrophages. Oxid Med Cell Longev 2015, 351827.
Wei, M., Chu, X., Jiang, L., Yang, X., Cai, Q., Zheng, C., Ci, X., Guan, M., Liu, J., Deng, X., 2012. Protocatechuic acid attenuates lipolysaccharide-induced acute lung injury. Inflammation 35, 1169–1178.
Wu, Y.X., Wu, T.Y., Xu, B.B., Xu, X.Y., Chen, H.G., Li, X.Y., Wang, G., 2016. Protocatechuic acid inhibits osteoclast differentiation and stimulates apoptosis in mature osteoclasts. Biomed. Pharmacother. 82, 399–405.
Yin, X., Zhang, X., Lv, C., Li, C., Yu, Y., Wang, X., Han, F., 2015. Protocatechuic acid ameliorates neurocognitive functions impairment induced by chronic intermittent hypoxia. Sci. Rep. 5, 14507.
Yune, T.Y., Lee, J.Y., Cui, C.M., Kim, H.C., Oh, T.H., 2009. Neuroprotective effect of Scutellaria baicalensis on spinal cord injury in rats. J. Neurochem. 110, 1276–1287.
Yune, T.Y., Lee, J.Y., Jiang, M.H., Kim, D.W., Choi, S.Y., Oh, T.H., 2008. Systemic administration of PEP-1-SOD1 fusion protein improves functional recovery by inhibition of neuronal cell death after spinal cord injury. Free Radic. Biol. Med. 45, 1190–1200.
Yune, T.Y., Lee, J.Y., Jung, G.Y., Kim, S.J., Jiang, M.H., Kim, Y.C., Oh, Y.J., Markelonis, G.J., Oh, T.H., 2007. Minocycline alleviates death of oligodendrocytes by inhibiting pro-nerve growth factor production in microglia after spinal cord injury. J. Neurosci. 27, 7751–7761.
Zhang, H.N., An, C.N., Zhang, H.N., Pu, X.P., 2010. Protocatechuic acid inhibits neurotoxicity induced by MPTP in vivo. Neurosci. Lett. 474, 99–103.
Zhang, N., Yin, Y., Xu, S.J., Wu, Y.P., Chen, W.S., 2012. Inflammation & apoptosis in spinal cord injury. Indian J. Med. Res. 135, 287–296.
Zhang, Z., Li, G., Szeto, S.S., Chong, C.M., Quan, Q., Huang, C., Cui, W., Guo, B., Wang, Y., Han, Y., Michael Siu, K.W., Yuen Lee, S.M., Chu, I.K., 2015. Examining the neuroprotective effects of protocatechuic acid and chrysin on in vitro and in vivo models of Parkinson disease. Free Radic. Biol. Med. 84, 331–343.
Zlokovic, B.V., 2008. The blood-brain barrier in health and chronic neurodegenerative disorders. Neuron 57, 178–201.